Structural Mimicry of Canonical Conformations in Antibody Hypervariable Loops Using Cyclic Peptides Containing a Heterochiral Diproline Template

Michel Favre, Kerstin Moehle, Luyong Jiang, Bernhard Pfeiffer, and John A. Robinson*

Contribution from the Institute of Organic Chemistry, University of Zürich, Winterthurerstrasse 190, 8057 Zürich, Switzerland

Received November 20, 1998. Revised Manuscript Received January 28, 1999

Abstract: Analyses of high resolution crystal structures have shown that antibody hypervariable loops L1, L2, and L3 from the light chain, as well as H1 and H2 from the heavy chain, can be assigned to only a small family of canonical conformations. We describe here attempts to generate structural mimetics of L2, L3, and H2 canonical conformations, which are β-hairpin structures connecting adjacent antiparallel β-strands. The five mimetics studied comprise cyclic peptides, in which the CDR loop has been transplanted from the immunoglobulin framework onto a D-Pro-L-Pro template. Their preferred conformations have been studied by NMR and MD with time-averaged, NOE-derived distance restraints. The results show that accurate mimetics of L3 and H2 loops can be obtained, whereas the L2 canonical conformation, which appears to be inherently strained, could not be mimicked in this way. For example, an eight-residue L3 loop from antibody HC19 attached to the D-Pro-L-Pro template adopts not only a backbone hairpin conformation but also aromatic−aromatic T-stacking interactions between tryptophan side-chains, that are essentially identical to those in the antibody crystal structure. This straightforward and effective approach to hairpin design may be of great value for generating small molecule mimetics of hairpin loops on proteins of diverse function.

Introduction

Interest in the design of peptide mimetics of surface patches on proteins involved in macromolecular recognition is growing rapidly,[1−3] not the least as a result of advances in genomic sciences and structural biology. In such endeavors it might be valuable to have available straightforward and effective methods for generating accurate conformational mimics of secondary structures, such as β-hairpins, in small synthetic molecules. β-Hairpins connect adjacent antiparallel β-strands,[4,5] occur on the surface of many proteins, and are frequently involved in protein−protein recognition. One example, par excellence, is found in the antigen binding sites on antibodies,[6] which are composed of amino acid residues located in six so-called hypervariable loops or complementarity-determining-regions (CDRs), three each from the heavy- and light-chain variable regions (V_H and V_L). In this work we show, to our knowledge for the first time, that accurate mimics of the allowed, so-called canonical conformations of antibody hypervariable loops can, at least in some cases, be easily generated using cyclic peptides constrained into a β-hairpin geometry by a heterochiral D-Pro-L-Pro dipeptide template. Moreover, the approach may be widely applicable to the design of β-hairpin mimetics, especially in the search for novel peptidomimetic drug or vaccine candidates.

Of the six CDR loops in antibodies of the IgG family, four may be classified as β-hairpins connecting adjacent antiparallel β-sheets, two from the V_L domain, L2 and L3, and two from the V_H domain, H2 and H3 (Figure 1). These variable loops, together with L1 and H1, are attached to the strands that together form the conserved framework structure of the antibody.[7] Recent estimates suggest that the large majority of L1, L2, L3, H1, and H2 hypervariable regions may be classified into one of 18 different canonical conformations.[8−11] Thus, although considerable sequence diversity may be accommodated in these loops, this is achieved within a restricted set of allowed conformations. The situation is more complex for the H3 loop, which not only accommodates the highest sequence diversity but also is more variable in length and conformation than the other CDR loops.[10,12−14] In this work, we have focused on the canonical conformations found in the L2, L3, and H2 β-hairpin loops, as

* Author to whom correspondence may be addressed. Telephone: (++)-41-1-635-4242. Fax: (++)-41-1-635-6812. E-mail: robinson@oci.unizh.ch.

(1) Cunningham, B. C.; Wells, J. A. *Curr. Opin. Struct. Biol.* **1997**, *7*, 457−462.
(2) KieberEmmons, T.; Murali, R.; Greene, M. I. *Curr. Opin. Biotechnol.* **1997**, *8*, 435−441.
(3) Reineke, U.; SchneiderMergener, J. *Angew. Chem., Int. Ed.* **1998**, *37*, 769−771.
(4) Sibanda, B. L.; Blundell, T. L.; Thornton, J. M. *J. Mol. Biol.* **1989**, *206*, 759−777.
(5) Sibanda, B. L.; Thornton, J. L. *Methods Enzymol.* **1991**, *202*, 59−82.
(6) Padlan, E. A. *Mol. Immunol.* **1994**, *31*, 169−217.
(7) Chothia, C.; Gelfand, I.; Kister, A. *J. Mol. Biol.* **1998**, *278*, 457−479.
(8) Chothia, C.; Lesk, A. M.; Tramontano, A.; Levitt, M.; Smith-Gill, S. J.; Air, G.; Sheriff, S.; Padlan, E. A.; Davies, D.; Tulip, W. R.; Colman, P. M.; Spinelli, S.; Alzari, P. M.; Poljak, R. J. *Nature* **1989**, *342*, 877−883.
(9) Chothia, C.; Lesk, A. M.; Gherardi, E.; Tomlinson, I. M.; Walter, G.; Marks, J. D.; Llewelyn, M. B.; Winter, G. *J. Mol. Biol.* **1992**, *227*, 799−817.
(10) Martin, A. C. R.; Thornton, J. M. *J. Mol. Biol.* **1996**, *263*, 800−815.
(11) Al-Lazikani, B.; Lesk, A. M.; Chothia, C. *J. Mol. Biol.* **1997**, *273*, 927−948.
(12) Morea, V.; Tramontano, A.; Rustici, M.; Chothia, C.; Lesk, A. M. *J. Mol. Biol.* **1998**, *275*, 269−294.
(13) Wu, T. T.; Johnson, G.; Kabat, E. A. *Proteins: Struct., Funct., Genet.* **1993**, *16*, 1−7.
(14) Shirai, H.; Kidera, A.; Nakamura, H. *FEBS Lett.* **1996**, *399*, 1−8.

10.1021/ja984016p CCC: $18.00
Published on Web 03/13/1999

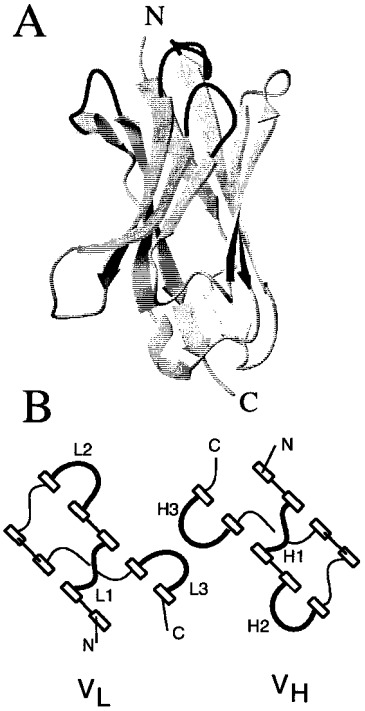

Figure 1. A, Ribbon diagram[36] of the V_H domain (only) of an antibody. The three CDR loops are at the top, in black. B, schematic view of the β-sheet sandwich seen in the V_H and V_L domains of an antibody. Each β-strand is represented by a rectangle. The CDRs are denoted by thick black lines and labeled L1−L3 and H1−H3. The N- and C-termini are also indicated.

determined in high-resolution crystal structures of antibody fragments. For the L2 region only a single canonical structure has been defined, whereas for L3 eight (six in V_κ and two in V_λ) and for H2 four different canonical structures have been described.[11]

To what extent are the canonical loop conformations influenced by contacts with the central framework region of the V-domains? This is certainly the case for the H1 and L1 loops, which pack across the top of each V-domain, bridging the two β-sheets, and each have near their center a hydrophobic side chain that packs in a cavity in the framework. Also, the influence of framework residues on the relative position of other loops within the antigen binding site has been noted, and the possibility of such effects must be borne in mind in attempts to create structural mimics of observed CDR structures.[9,11,15,16]

To create β-hairpin mimetics we have used the structurally well-defined[17−19] heterochiral D-Pro-L-Pro dipeptide as a template to fix the N- and C-terminal residues of the loop in the same geometry found in adjacent β-strands of the intact protein. Several heteroaromatic templates such as **1**−**3**[20,21] and diketopiperazine-based templates such as **4** and **5**[22,23] have been described that promote β-sheet and β-hairpin formation. For this study, however, the D-Pro-L-Pro dipeptide template was chosen, since this uses commercially available building blocks, and was shown in earlier work to stabilize β-hairpin structures in aqueous solution in a loop mimetic derived from a cytokine receptor.[24]

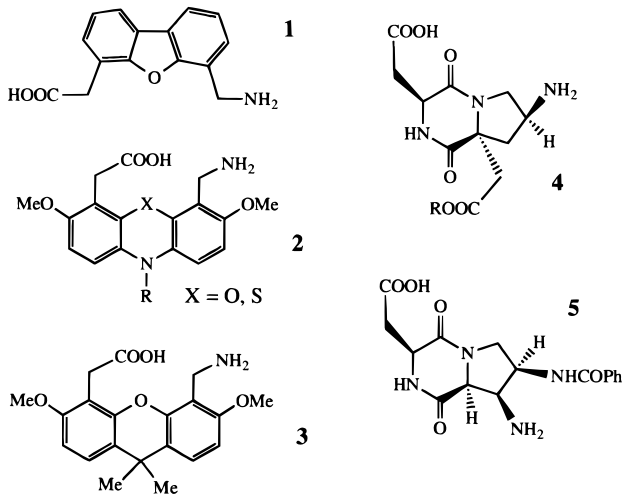

Results and Discussion

Design and Synthesis. We have not attempted a systematic study of all known canonical structures, but rather have tried to select representative examples, and these are listed in Table 1. The D-Pro-L-Pro template is known to strongly prefer a type-II′ β turn backbone conformation.[17−19,24] Using this information, mimetic design involved transplanting the loop sequence by computer modeling from the antibody to the template, such that the correct directional register of the peptide amide bonds in the backbone is maintained, as depicted for mimetic **10** in Figure 2.

The target peptides **6**−**10** were synthesized in two stages. The linear side-chain protected peptides were first assembled by solid-phase synthesis using Fmoc chemistry,[25] such that the D-Pro-L-Pro unit is incorporated near the middle of the sequence, and then cyclization was performed in solution. Cyclization was monitored by HPLC and in all cases proceeded in >90% yield.

Conformational Analysis. General. Conformational analyses were carried out by NMR spectroscopy and molecular dynamics (MD) simulations. The ^{1}H NMR spectra of **6**−**10** each showed only a single major species on the chemical shift time scale. ^{1}H NMR assignments were achieved by standard methods[26] (see Supporting Information, Tables 1S−5S). In all cases, the 1D ^{1}H NMR spectra showed no significant changes in shifts or line widths over the concentration range ca. 30−0.2 mM. The solution conformations of **6** and **9** were studied in water at pH 5.0, whereas **7**, **8**, and **10** were poorly water soluble and thus were studied in DMSO. As shown below, the three peptides **7**, **8** and **10** studied in DMSO bear remarkable structural similarities to their corresponding H2 and L3 canonical conformations in the parent antibody crystal structures, whereas the peptides

(15) Tomlinson, I. M.; Walter, G.; Marks, J. D.; Llewelyn, M. B.; Winter, G. *J. Mol. Biol.* **1992**, *227*, 776−798.
(16) Tomlinson, I. M.; Cox, J. P. L.; Gherardi, E.; Lesk, A. M.; Chothia, C. *EMBO J.* **1995**, *14*, 4628−4638.
(17) Bean, J. W.; Kopple, K. D.; Peishoff, C. E. *J. Am. Chem. Soc.* **1992**, *114*, 5328−5334.
(18) Nair, C. M.; Vijayan, M.; Venkatachalapathi, Y. V.; Balaram, P. *J. Chem. Soc., Chem. Commun.* **1979**, 1183−1184.
(19) Chalmers, D. K.; Marshall, G. R. *J. Am. Chem. Soc.* **1995**, *117*, 5927−5937.
(20) Tsang, K. Y.; Diaz, H.; Graciani, N.; Kelly, J. W. *J. Am. Chem. Soc.* **1994**, *116*, 3988−4005.
(21) Müller, K.; Obrecht, D.; Knierzinger, A.; Stankovic, C.; Spiegler, C.; Bannwarth, W.; Trzeciak, A.; Englert, G.; Labhardt, A. M.; Schönholzer, P. In *Perspectives in Medicinal Chemistry*; Testa, B., Kyburz, E., Fuhrer, W., Giger, R., Eds.; Verlag Helv. Chim. Acta: Basel, 1993; pp 513−531.
(22) Pfeifer, M. E.; Robinson, J. A. *J. Chem. Soc., Chem. Commun.* **1998**, 1977−1978.
(23) Bisang, C.; Jiang, L.; Freund, E.; Emery, F.; Bauch, C.; Matile, H.; Pluschke, G.; Robinson, J. A. *J. Am. Chem. Soc.* **1998**, *120*, 7439−7449.
(24) Späth, J.; Stuart, F.; Jiang, L.; Robinson, J. A. *Helv. Chim. Acta* **1998**, *81*, 1726−1738.
(25) Atherton, E.; Sheppard, R. C. *Solid-phase peptide synthesis-a practical approach*; IRL Press: Oxford, 1989.
(26) Wüthrich, K. *NMR of Proteins and Nucleic Acids*; Wiley-Interscience: New York, 1986.

Table 1. Sequences of Hairpin Loops[a]

no.	hairpin type	sequence (mimetic)	antibody (pdb code)	resolution (Å)	canonical conformation
1	3:3	YRDAM (**6**)	KOL (2fb4)	1.90	L2
2	3:5	FYTGT (**7**)	NEWM (7fab)	2.00	H2.1
3	4:6	NTYSGV (**8**)	TE33 (1tet)	2.30	H2.2
4	4:6	WDDGSD (**9**)	KOL (2fb4)	1.90	H2.3
5	2:4	LWYSNHWV (**10**)	HC19 (1gig)	2.30	λL3.1

[a] Hairpin type seen in the crystal structure using the classification system of Sibanda et al.,[4,5] the Brookhaven Protein Data Bank (pdb) code for the antibody crystal stucture and its resolution, and the canonical conformation according to Chothia[8,9,11]

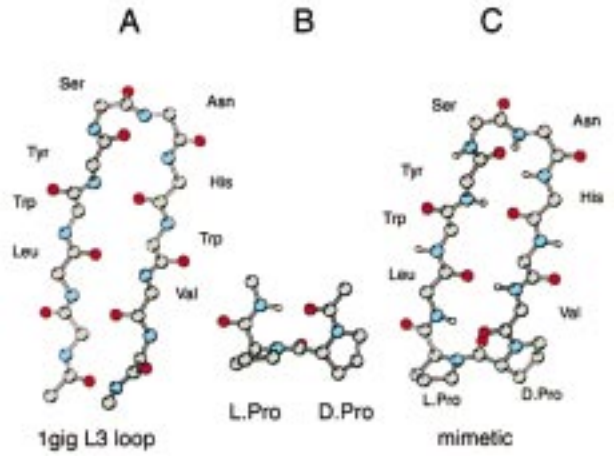

Figure 2. A, shows the backbone of the L3 loop of the anti-influenza hemagglutinin antibody HC19[37,38] from PDB file 1gig. B, the preferred conformation of the D-Pro-L-Pro template. **C**, transplanting the loop from Leu[92] to Val[99] to the template creates the mimetic **10**.

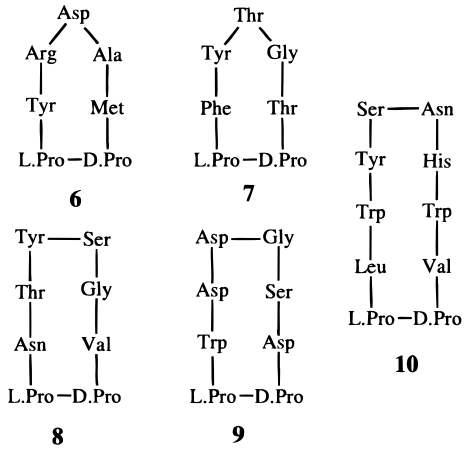

6 and **9** are poorer mimics of their corresponding L2 and H2 canonical loop conformations.

Apart from NOEs, three parameters are often used as indicators of stable secondary structure in peptides; $^3J_{HNH\alpha}$ coupling constants, which lie in the range 6−8 Hz in a random coil peptide, but are <6 Hz in helices and >8 Hz in β-sheets; amide proton temperature coefficients, which are typically smaller (less negative) than −4 to −5 ppb/K for an amide that is shielded from solvent; and relative H/D exchange rates of amide protons, which are considerably slowed when the NH is involved in strong intramolecular hydrogen bonding or otherwise shielded from solvent. These parameters were determined for **6**−**10** and are collected in Figure 3. Note that the lowest observed temperature coefficients do not always correlate with the slowest relative exchange rates. The relative H/D exchange rates are more easily interpretable, since a relatively slow exchange unequivocally indicates intramolecular H-bonding and/or shielding of the NH proton from solvent. All of the peptides show at least one peptide NH that exchanges very slowly; for example, in peptide **10** the Leu[1], Tyr[3], and Val[8] NHs show half-lives for exchange in d_6-DMSO + 10% d_4-MeOH of ca. 12 days at 305 K, whereas the Asn[5] NH has a half-life of ca. 10 min.

Some of the observed NOE connectivities for **6**−**10** are shown in Figure 3, and other long-range NOEs (i.e., between nonneighboring residues) are indicated in Figure 4. The large number of long-range NOEs observed in NOESY spectra of **10** is exceptional and provide strong a priori evidence for a stable hairpin structure. For each peptide, the NOE connectivities were used to derive upper distance restraints for structure calculations using dynamic simulated annealing[27] (SA). No dihedral angle restraints were used in SA calculations, since NOEs and coupling constants are influenced in different ways by conformational averaging. The structures obtained by SA calculations were inspected for their relatedness to each other (i.e., convergence) and to the crystal structures of the corresponding CDR loops in the antibodies. In addition, a representative SA structure was used as a start for MD simulations with time-averaged distance restraints[28,29] (TA-DR) and explicit DMSO or water solvent molecules present (Tables 2 and 3), i.e., the atom−atom upper distance restraints are introduced as values that are to be fulfilled, not instantaneously, but over the course of an MD simulation with solvent present. The use of time-averaged restraints in this way, has been proposed[28,29] as one means to take into account, in structure calculations, the averaging that is inherent in NMR spectroscopic data.

It should be noted that it is essentially impossible here to fully and accurately describe the dynamics of these mimetics, since they are flexible molecules most likely undergoing complex motional behavior. The SA calculations, however, should provide to a first approximation a good indication of their preferred solution structures and hence their overall similarity to the canonical structures in the intact antibodies. In addition, the MD simulations may provide insights into the extent of conformational averaging experienced by each peptide on the MD time scale. The results are discussed below.

Peptide 10. The ensemble of SA structures calculated for **10** converge to a family of closely related β-hairpin conformations (Figure 5A). This convergence appears to derive from the large number of distance restraints used in the calculations, many being long range and highly indicative of a hairpin conformation (Figure 4), as well as from the intrinsic stability of an eight-residue hairpin loop attached to the D-Pro-L-Pro template. The β-hairpin remains stable in both restrained (Table 3) (with TA-DR) and unrestrained (data not shown) 2.0 ns MD simulations, with mostly small fluctuations in backbone ϕ and ψ angles. The three backbone peptide NH groups (for Leu[1], Tyr[3], and Val[8]), apparent in the SA structures and by MD, that participate in H-bonding across the hairpin are also those that have the slowest H/D exchange rates (Figures 3 and 5A). There is convincing evidence from NOE connectivities for the presence of T-stacking involving the indole rings of Trp[2] and Trp[7] in **10** (Figure 5A). CD Spectra of **10** in MeOH and in 10% MeOH−H_2O both showed a strong exciton couplet at 225 nm (DMSO

(27) Nilges, M.; Gronenborn, A. M.; Brünger, A. T.; Clore, G. M. *Protein Eng.* **1988**, *2*, 27−38.
(28) Torda, A. E.; Scheek, R. M.; van Gunsteren, W. F. *Chem. Phys. Lett.* **1989**, *157*, 289−294.
(29) Nanzer, A. P.; Vangunsteren, W. F.; Torda, A. E. *J. Biomol. NMR* **1995**, *6*, 313−320.

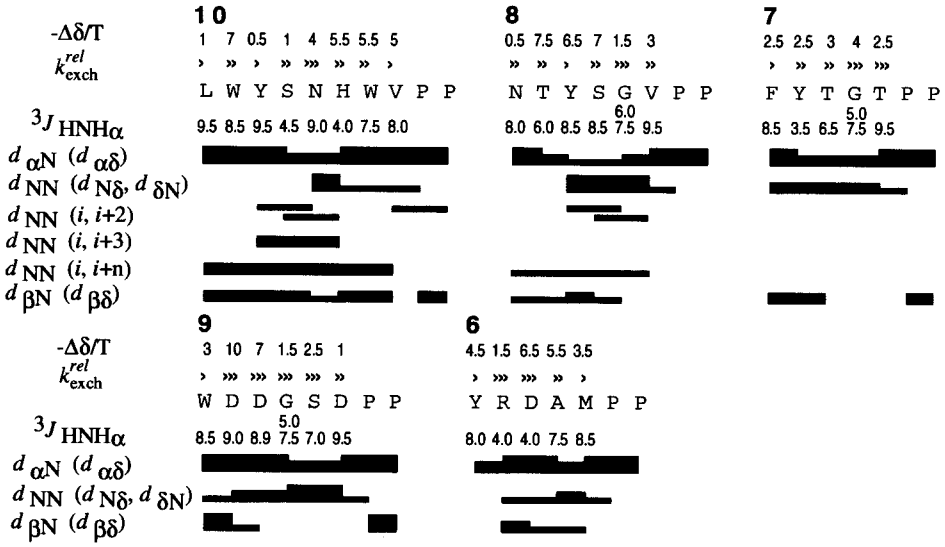

Figure 3. The temperature coefficients ($-\Delta\delta/T$) in ppb/K (determined over the range 280−315 K, or 295−325 K, for aqueous and DMSO solutions, respectively); relative H/D exchange rates of peptide NH protons (> slow, ≫ medium, >>> fast) (determined by monitoring residual peak intensities after dissolution in d_6-DMSO + 10% d_4-MeOH, or in D_2O (pD* 3.5), as appropriate); backbone $^3J_{HNH\alpha}$ coupling constants determined in 1D spectra; and NOE connectivities (thick line = strong, medium line = medium, thin line = weak) measured for the mimetics **6**−**10**.

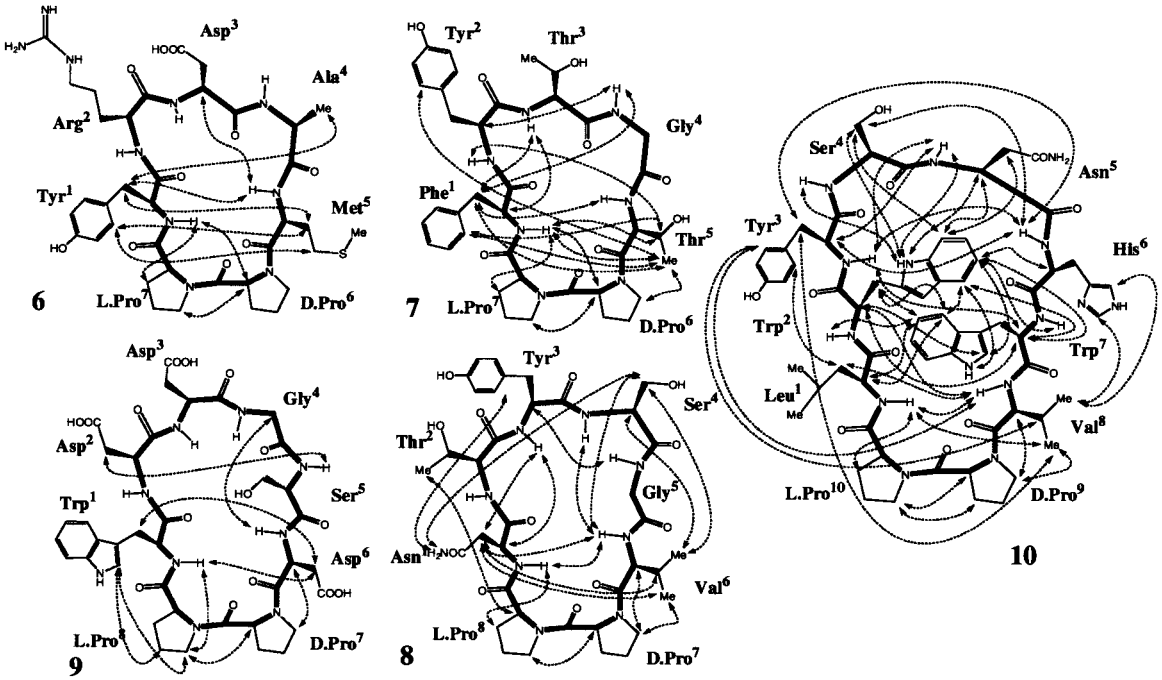

Figure 4. Other key NOE connectivities found for mimetics **6**−**10**, each indicated by a dotted arrow.

Table 2. Results from MD Simulations with Time-Averaged Distance Restraints for the Mimetics **6**−**10**

TA-DR	FYTGT (**7**)	NTYSGV (**8**)	LWYSNHWV (**10**)	YRDAM (**6**)	WDDGSD (**9**)
no. of solute atoms	72	73	122	73 (+2 Ions)	75 (+3 Ions)
no. of solvent molecules	286 (DMSO)	344 (DMSO)	339 (DMSO)	1030 (H_2O)	1060 (H_2O)
distance restraint energy (kJ/mol)	19.8 ± 4.4	7.2 ± 1.9	32.7 ± 5.1	6.5 ± 2.9	5.7 ± 2.1
temperature (K)	300.2 ± 5.5	300.3 ± 5	300.0 ± 4.9	302.4 ± 3.2	302.6 ± 3.9
sum of positive violations of distance restraints (Å), and number of restraints	5.21 (52)	4.08 (37)	15.68 (110)	1.85 (28)	3.7 (26)
average violation (Å)	0.1	0.11	0.14	0.07	0.14
rms of violations (Å)	0.39	0.23	0.25	0.24	0.15
range of violations (Å)	0.03−1.36	0−0.85	0.02−1.11	0.03−0.67	0.07−0.45

has a strong UV absorbance which precludes analysis of CD spectra), indicating that the two indole rings interact in close proximity also in these solvents. Whether or not this interaction contributes significantly to the stability of the hairpin is presently less clear.

Upon comparison to the L3 loop in the crystal structure of the antibody, the backbone conformation and all side-chain positions, including the T-stacked arrangement of the Trp^2 and Trp^7 indole rings, are found to be very similar to those in a typical SA structure of **10** (Figure 6A). The L3.1 canonical

Table 3. ϕ and ψ Angles for Each Residue in the CDR Loop[a]

	cryst	SA	MD		cryst	SA	MD
(**6**) $Y_1R_2D_3A_4M_5$				(**9**) $W_1D_2D_3G_4S_5D_6$			
ϕ_1	−118.0	−74.4	−94.7 ± 27.0	ϕ_1	−59.4	−107.9	−74.3 ± 25.1
ψ_1	157.9	148.9	144.1 ± 17.3	ψ_1	158.2	118.7	147.2 ± 15.7
ϕ_2	47.7	−66.1	−55.9 ± 15.7	ϕ_2	−41.4	57.7	51.4 ± 12.0
ψ_2	57.3	145.5	−19.3 ± 52.7	ψ_2	−48.0	61.8	62.4 ± 17.4
ϕ_3	70.6	75.7	−107.6 ± 61.6	ϕ_3	−100.0	50.5	49.5 ± 13.5
ψ_3	−54.0	66.8	93.5 ± 32.0	ψ_3	6.4	61.6	41.0 ± 32.9
ϕ_4	−142.9	43.5	48.3 ± 36.9	ϕ_4	70.8	78.6	87.7 ± 36.3
ψ_4	0.7	60.3	−15.1 ± 38.2	ψ_4	14.7	2.0	6.3 ± 30.3
ϕ_5	−80.4	−148.4	−111.3 ± 28.7	ϕ_5	−70.4	−68.8	−73.0 ± 22.4
ψ_5	150.0	74.6	104.5 ±17.6	ψ_5	−16.4	−43.1	−41.2 ± 13.0
(**7**) $F_1Y_2T_3G_4T_5$				ϕ_6	−156.6	−136.2	−121.4 ± 12.2
ϕ_1	−101.4	−37.2	−85.1 ± 21.6	ψ_6	155.6	86.0	84.8 ± 10.6
ψ_1	155.8	139.5	163.8 ± 42.1	(**10**) $L_1W_2Y_3S_4N_5H_6W_7V_8$			
ϕ_2	−62.7	−67.8	−78.2 ± 32.2	ϕ_1	−127.2	−108.1	−107.2 ± 20.9
ψ_2	−26.8	−0.2	−19.5 ± 32.2	ψ_1	136.2	121.6	140.0 ± 15.6
ϕ_3	−70.6	−119.5	−90.9 ± 26.1	ϕ_2	−92.2	−84.2	−92.9 ± 16.4
ψ_3	−15.3	24.5	20.8 ± 27.9	ψ_2	132.3	118.7	134.9 ± 11.2
ϕ_4	111.7	75.5	84.6 ± 36.2	ϕ_3	−125.2	−102.5	−128.2 ± 12.9
ψ_4	−11.1	24.8	20.1 ± 37.7	ψ_3	64.3	161.5	88.5 ± 17.9
ϕ_5	−57.0	−100.1	−110.0 ± 30.5	ϕ_4	58.2	−52.3	53.2 ± 18.3
ψ_5	131.5	88.7	84.9 ± 15.4	ψ_4	−35.7	−22.6	−51.4 ± 15.4
(**8**) $N_1T_2Y_3S_4G_5V_6$				ϕ_5	−130.7	−136.5	−124.1 ± 14.7
ϕ_1	−72.4	−94.7	−99.7 ± 29.5	ψ_5	−8.7	17.9	−20.7 ± 16.0
ψ_1	114.8	108.4	105.8 ± 15.4	ϕ_6	−150.3	−159.6	−141.4 ± 15.7
ϕ_2	−72.8	−90.7	−72.2 ± 15.4	ψ_6	163.9	147.9	159.3 ± 11.9
ψ_2	−16.7	66.9	−32.1 ± 11.0	ϕ_7	−106.7	−88.5	−85.1 ± 13.7
ϕ_3	−79.6	−156.9	−61.9 ± 11.6	ψ_7	145.8	136.2	134.8 ± 11.6
ψ_3	−58.9	−72.1	−44.4 ± 12.6	ϕ_8	−132.6	−107.7	−118.9 ± 11.2
ϕ_4	−75.2	−74.6	−89.3 ± 16.7	ψ_8	125.3	88.8	91.2 ± 9.4
ψ_4	−16.2	−33.0	−26.6 ± 18.6				
ϕ_5	70.8	90.5	86.8 ± 21.0				
ψ_5	8.8	49.3	27.1 ± 24.1				
ϕ_6	−90.4	−127.5	−117.3 ± 19.1				
ψ_6	121.9	87.7	105.4 ± 13.8				

[a] (a) In the crystal structure (see Table 1 for pbd entry), (b) in the SA structure of the mimetics (**6**−**10**) used for MD simulations, and (c) the averages and rms deviations over the course of the 2ns simulations of the mimetics (**6**−**10**) with TA-DR.

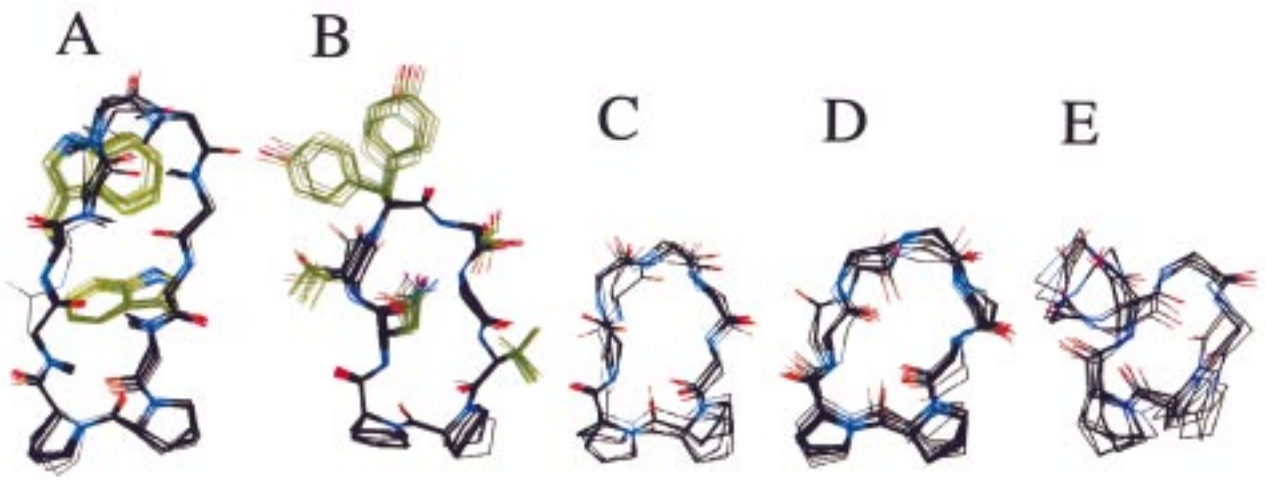

Figure 5. Superimpositions over all backbone N, Cα, and C atoms of the structures calculated by SA using NOE-derived distance restraints. All structures within 20 kcal/mol of the minimum energy structure and showing no distance violations >0.3 Å were used for the superimpositions. O-atoms are in red, N-atoms in blue, and side chains in green. A for **10**; B for **8**; C for **7**; D for **6**; and E for **9**.

conformation of this antibody, therefore, seems to be intrinsically stable outside the context of the Ig fold and is well mimicked in the cyclic peptide **10**.

Peptide 8. Although fewer long-range NOEs are seen for **8** than for **10** (Figures 3 and 4), the SA structures again converge to a family of closely related backbone conformers (Figure 5B), which are very similar to that found in the H2.2 canonical conformation in the antibody (Figure 6B). This backbone conformation was maintained with mostly small fluctuations of ϕ and ψ angles in the restrained MD simulation, with the exception of ψ_2 and ϕ_3, i.e., the Thr^2-Tyr^3 amide plane (Table 3), which quickly adjusts during the simulation to that seen in the antibody crystal structure. The Tyr^3 NH exchanges relatively slowly in **8**. This is not well accounted for by H-bonding during the MD simulations, although a γ-turn from Tyr^3 NH to the Asn^1 CO is observed in the SA structures (Figure 5B). Since the loop comprises six rather than eight residues, a backbone hairpin conformation different to that seen in **10** is unavoidable

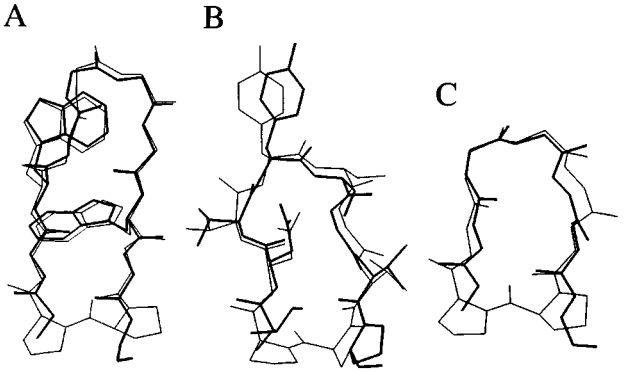

Figure 6. Superimpositions of the SA structure used for MD simulations (thin lines) with the CDR loop structure from the antibody crystal structure (thick lines); A for mimetic **10** and the L3 loop from the HC19 Fab; B for mimetic **8** and the H2 loop from antibody TE33; C for mimetic **7** and the H2 loop from the antibody NEWM (see Table 1).

(see Design and Synthesis). The glycine at position-5 adopts ϕ/ψ angles of $\sim+90/+30$, which would not be favorable for a non-glycine residue at this position; therefore, its presence and location in the loop may be important for the stability of the backbone conformation found.

We conclude that the mimetic **8** displays flexibility, e.g., in reorientations of peptide planes and side-chain torsional angles. The H2.2 canonical conformation, however, seems to be intrinsically stable outside the context of the Ig fold and, within the limited accuracy of the structure calculations, appears to be well mimicked by **8** (Figure 6B).

Peptide 7. The NH resonances of Tyr^2 and Gly^4, and to a lesser extent also Thr^3 and Thr^5 (but not Phe^1), are slightly broadened in DMSO at 300 K. These NH signals sharpen, however, as the temperature is raised to 335 K, consistent with the broadening arising from conformational exchange. ROESY spectra at 335 K and NOESY spectra at 300 K were each used to derive distance restraints, and SA calculations with each data set gave similar results. The NOE connectivities between Phe^1 and Thr^5 in peptide **7** (Figure 4) indicate again the influence of the D-Pro-L-Pro template in stabilizing a β-hairpin. The SA structures obtained seem to cluster into two main families of backbone conformers (Figure 5C), which differ mainly in the orientation of the Phe^1-Tyr^2 and Tyr^2-Thr^3 peptide planes. The most frequently observed conformer is very similar to the H2.1 canonical conformation in the antibody 7fab (Figure 6C). The fluctuations in ϕ and ψ angles observed for **7** during the restrained MD simulation are greater, however, than was the case for **8** and **10** (Table 3). A Phe^1 NH to Thr^5 CO H-bond is the one most frequently populated in the restrained MD simulation, which is consistent with this NH being the slowest to exchange (Figure 3), with a half-life of about 30 h in DMSO with 10% d_4-methanol.

These results indicate that although the mimetic **7** does not adopt a single major backbone geometry, conformations very similar to that in the H2.1 canonical structure are populated under the conditions studied.

Peptides 6 and 9. Whereas long-range NOEs between the amino acids directly attached to the D-Pro-L-Pro template are again observed for **6** and **9**, the total number is now reduced, and very few are observed involving residues at the tip of each loop (Figure 4). For both **6** and **9** the SA calculations do not generate a single family of backbone conformers (Figure 5D and E), and none of those observed are similar to the canonical conformations in the antibody crystal structures.

In the case of **6**, there is considerable diversity in the orientation of peptide planes connecting Tyr^1, Arg^2, and Asp^3. This is also reflected in the restrained MD simulation (Table 3), where ϕ and ψ angles undergo much larger fluctuations and exhibit significant differences from the crystal conformation. The single L2 canonical conformation found in the V_λ and V_κ domains of at least 16 antibodies determined at high resolution[11] form a three-residue hairpin loop joining framework residues 49 and 53. This three-residue loop adopts a γ-turn with ϕ/ψ angles for residue 51 at the tip of the loop in a strained conformation (Table 3). This corresponds to Asp^3 in **6**. Thus, the ubiquitous L2 canonical conformation appears to be stabilized by contacts it makes within the intact V_L domain, it does not correspond to an intrinsically stable loop conformation, and most likely for this reason it is not mimicked in the cyclic peptide **6**.

The structures deduced by SA for **9** adopt a folded hairpin-like structure, whose backbone traces a path resembling the seam of a tennis ball (Figure 5E). This is most unlike the H2.3 canonical conformation found in antibody KOL (Table 1) and is also unlike the conformations deduced for the backbone of **8**, which has the same hairpin length. The ϕ/ψ angles of Asp^2-Asp^3 in **9** adopt predominantly a left-handed helical structure in the MD simulation, whereas a βI-turn conformation is seen in the antibody crystal structure. We conclude, therefore, that this CDR backbone conformation is not accurately mimicked in **9**, for reasons that are presently not certain. In other words, despite the hairpin-inducing properties of the D-Pro-L-Pro template, the length and sequence of the loop have a strong influence on its preferred conformation, according to rules that have yet to be defined.

Conclusions

Cyclic peptides containing a heterochiral diproline are an interesting class of protein loop mimetics, due to the strong β-hairpin inducing properties of the D-Pro-L-Pro template. This conclusion has been confirmed and its generality extended in the present work, in loops of varying length and sequence. This class of cyclic peptides can be made efficiently, using commercially available building blocks and standard solid-phase and solution synthesis methods. Here we have shown that the allowed canonical conformations of CDR loops observed in high resolution crystal structures of antibody fragments can, at least in some cases, be accurately reproduced in cyclic peptides containing a D-Pro-L-Pro template. For example, the eight-residue L3 loop from antibody HC19 attached to the D-Pro-L-Pro template, adopts a backbone conformation very similar to that in the antibody, and even aromatic−aromatic T-stacking interactions between tryptophan side chains located on opposite sides of the hairpin are faithfully reproduced in the cyclic peptide mimetic. In the case of the L2 canonical loop, however, the backbone conformation in the antibody appears to be strained and stabilized by contacts made in the context of the intact immunoglobulin fold; the same loop mounted on the D-Pro-L-Pro template adopts quite different backbone conformations.

The results reported here may have practical value in the design of biologically active small-molecule protein loop mimetics, given the ease of synthesis and β-hairpin mimicry of D-Pro-L-Pro-containing cyclic peptides. For example, there have been many reports of CDR mimetics that retain some, albeit low, affinity for the antigen bound by the intact antibody.[2,30] The backbone conformation of the CDR almost certainly plays

(30) Smythe, M. L.; Vonitzstein, M. *J. Am. Chem. Soc.* **1994**, *116*, 2725−2733.

a key role in accurately positioning residues for interaction with the antigen. On the other hand, crystallographic and mutagenesis studies on antibody−protein antigen complexes have revealed that residues in several CDR loops typically provide energetically important contacts with the bound protein antigen.[31] The invention of small molecules that mimic multiple CDR loops is currently also attracting attention,[32] and D-Pro-L-Pro-containing cyclic peptides may be interesting building blocks for this purpose. Alternatively, so-called heavy-chain camelid antibodies have been found, which lack a light chain and use long CDR H3 loops to fill cavities on protein antigens.[33] Hairpin structures on other immunoglobulin-like proteins, as well as in many other classes of protein fold, are also known to mediate the biological activity of the intact protein[2]. Hence, β-hairpin mimetics based upon cyclic peptides containing the D-Pro-L-Pro template might prove to be of general use as a starting point in protein ligand, vaccine, and receptor antagonist design.

Experimental Section

General. DMF was dried over $MgSO_4$ and redistilled from ninhydrin just prior to use. High performance liquid chromatography (HPLC) was carried out using a dual pump Pharmacia system with Waters RCM-μBondapak-C_{18} cartridges (10 μm, 300 Å, 25 × 100 mm) for preparative and (8 × 100 mm) analytical separations, with flow rates of 8 mL/min and 2 mL/min, respectively. UV-detection was at 226 and 278 nm.

Peptide Synthesis. Typically, the first amino acid was coupled to Tentagel-S AC resin (Rapp Polymere, Tübingen) in CH_2Cl_2 and pyridine (1:1) using 2-chloro-1,3-dimethylimidazolidinium hexafluorophosphate (6 equiv) for 1 h. The following linear peptide chains were then assembled using standard Fmoc-chemistry[25] in DMF

H-Ala-Met-D-Pro-L-Pro-Tyr(*t*Bu)-Arg(Pmc)-Asp(*t*Bu)-O−RESIN

H-Gly-Thr(*t*Bu)-D-Pro-L-Pro-Phe-Tyr(*t*Bu)-Thr(*t*Bu)-O−RESIN

H-Ser(*t*Bu)-Gly-Val-D-Pro-L-Pro-Asn(Mtt)-Thr(*t*Bu)-Tyr(*t*Bu)-O−RESIN

H-Gly-Ser(*t*Bu)-Asp(*t*Bu)-D-Pro-L-Pro-Trp(Boc)-Asp(*t*Bu)-Asp(*t*Bu)-O−RESIN

H-Asn(Mtt)-His(Trt)-Trp(Boc)-Val-D-Pro-L-Pro-Leu-Trp(Boc)-Tyr(*t*Bu)-Ser(*t*Bu)-O−RESIN

Each linear peptide was cleaved from the resin with 1% TFA in CH_2Cl_2 and purified by HPLC. The linear precursor was cyclized at a concentration of ca. 1 mg/mL in DMF using HATU (3 equiv), HOAt (3 equiv), and DIEA (0.6% v/v). The protected cyclic peptide was purified by HPLC. Side-chain protecting groups were removed with either TFA/triisopropylsilane:H_2O (95:2.5:2.5) or (for **6**) TFA/triisopropylsilane/ethanedithiol/water (92.5:2.5:2.5:2.5), the product was precipitated with diisopropyl ether, and purified by HPLC. EI-MS (**6**): 831 ([M + H]$^+$); EI-MS (**7**): 786 ([M + Na]$^+$), 764 ([M + H]$^+$); EI-MS (**8**): 839 ([M + Na]$^+$), 816 ([M + H]$^+$); EI-MS (**9**): 893 ([M + Na]$^+$), 871 ([M + H]$^+$); EI-MS (**10**): 1281 ([M + H]$^+$).

NMR and Structure Calculations. ^{1}H 1D and 2D NMR spectra were recorded at 600 MHz (Bruker AMX600 spectrometer), typically at a peptide concentration of ~20 mg/mL, for **6** and **9** in H_2O/D_2O (90:10), pH 5, and for **7**, **8**, and **10** in d_6-DMSO. The water signal was presaturated. Two-dimensional spectra were analyzed using Felix software (MSI, San Diego).

To derive NOE distance restraints it was assumed that the initial rate approximation is valid and that each peptide rotates as a single isotropic rotor. The NOEs were determined from NOESY and/or ROESY spectra measured with mixing times of 40, 80, 120, and 250 ms, with 2048 × 512 data points and zero-filling to 4096 × 2048, and transformed with a sine-bell weighting function. For **7** a NOESY series at 300 K and ROESY series at 335 K, for **9** ROESY at 300 K and NOESY at 278 K, for **6** ROESY at 300 K, for **8** NOESY spectra at 300 K, and for **10** NOESY spectra at 305 K were measured. Cross-peak volumes were determined by integration, and the build-up curves were checked to ensure a smooth exponential increase in peak intensity for all NOEs used in deriving distance restraints. The relative cross-peak volumes were assumed to be proportional to r^{-6} and were used to derive distance restraints for simulated annealing (SA) calculations, performed using methods described in detail elsewhere.[34]

For MD simulations with and without TA-DR the GROMOS96 suite of programs[35] was used with the 43A1 force field. Arg and Asp residues were simulated with charged side chains and Na^+ or Cl^- counterions to ensure electrical neutrality. The upper distance restraints were the exact values obtained from NOE build-up curves, where necessary with pseudoatom corrections, a memory decay time $\tau_{dr} = 50$ ps, and a force constant $K_{dr} = 1000$ kJ mol^{-1} nm^{-2}. The starting structure was one of the lowest energy SA structures embedded in a truncated octahedral box filled with either SPC water or DMSO molecules. The temperature was held constant by weak coupling ($\tau_T = 0.1$ ps) to an external bath at 300 K. The SHAKE algorithm was used to maintain bond lengths with a relative precision of 10^{-4} and the integrator time step was 0.002 ps. Nonbonded interactions evaluated at every step were within a short-range cutoff of 8 Å (or 9 Å for DMSO). For long-range interactions, calculated every five steps, the cutoff was 14 Å (15 Å for DMSO). Structures were saved for analysis every 100 steps (0.2 ps). After short simulations to relax the solute and solvent, the simulations with and without TA-DR were each run for 2 ns.

Acknowledgment. This work was supported by grants from the Swiss National Science Foundation. The authors thank Professor Wilfred van Gunsteren (ETH-Z) for the GROMOS96 suite of programs.

Supporting Information Available: Five tables of ^{1}H NMR assignments (PDF). This material is available free of charge via the Internet at http://pubs.acs.org.

JA984016P

(31) Davies, D. R.; Cohen, G. H. *Proc. Natl. Acad. Sci. U.S.A.* **1996**, *93*, 7−12.

(32) Hamuro, Y.; Calama, M. C.; Park, H. S.; Hamilton, A. D. *Angew. Chem., Int. Ed. Engl.* **1997**, *36*, 2680−2683.

(33) Lauwereys, M.; Ghahroudi, M. A.; Desmyter, A.; Kinne, J.; Holzer, W.; DeGenst, E.; Wyns, L.; Muyldermans, S. *EMBO J.* **1998**, *17*, 3512−3520.

(34) Bisang, C.; Weber, C.; Robinson, J. A. *Helv. Chim. Acta* **1996**, *79*, 1825−1842.

(35) van Gunsteren, W. F.; Billeter, S. R.; Eising, A. A.; Hünenberger, P. H.; Krüger, P.; Mark, A. E.; Scott, W. R. P.; Tironi, I. G. *Biomolecular simulation: The GROMOS96 manual and user guide*; Hochschulverlag AG an der ETH Zürich: Zurich, 1996.

(36) Koradi, R.; Billeter, M.; Wüthrich, K. *J. Mol. Graphics* **1996**, *14*, 51−55.

(37) Bizebard, T.; Daniels, R.; Kahn, R.; Golinelli-Pimpaneau, B.; Skehel, J. J.; Knossow, M. *Acta Crystallogr.* **1994**, *D50*, 768−777.

(38) Bizebard, T.; Gigant, B.; Rigolet, P.; Rasmussen, B.; Diat, O.; Bösecke, P.; Wharton, S. A.; Skehel, J. J.; Knossow, M. *Nature* **1995**, *376*, 92−94.